Materials Science, *Vol. 21*, *No. 1*, *2003*

Magnetic properties of Fe/Si and Co/Si multilayers

T. LUCIŃSKI[1, 3*], M. KOPCEWICZ[2], A. HÜTTEN[3],
H. BRÜCKL[3], S. HEITMANN[3], T. HEMPEL[3], G. REISS[3]

[1]Institute of Molecular Physics, Polish Academy of Sciences,
Smoluchowskiego 17, 60-172 Poznań, Poland

[2]Institute of Electronic Materials Technology, Warsaw, Poland

[3]Faculty of Physics, University of Bielefeld, Bielefeld, Germany

Magnetic and structural properties of Fe/Si, Fe/$Fe_{33}Si_{66}$ and Co/Si multilayers have been studied. Very strong AF coupling $J = -1.93$ mJ/m^2 accompanied by saturation field of 1.5 T has been found for d_{Si} = 1.4 nm. The CEMS spectra recorded at room temperature consist of the Zeeman sextet characteristic of the pure Fe phase accompanied by two spectral components related to FeSi system: magnetic broad sextet and a quadrupole doublet. The broad sextet could originate from various Fe sites at the interface. The nonmagnetic QS doublet is most probably associated with the nonstoichiometric c-$Fe_{1-x}Si_x$ phase. Comparing the results obtained for Fe/Si and Fe/$Fe_{33}Si_{66}$ multilayers we conclude that the exchange coupling is distinctly stronger for nominally pure spacer layer. For Co/Si multilayers a very weak antiferromagnetic coupling and oscillatory $F_{AF}(d_{Si})$ behaviour was observed, most probably due to the formation of Co–Si nonmagnetic metallic phases replacing the nominally pure Si spacer layers. We have shown that AF coupled Fe/Si multilayers can be successfully applied as an antiferromagnets in the magnetoresistive $(Fe/Si)_{15}$/Fe/Co1/Cu/Co2 system.

Key words: *multilayers, interlayer coupling, magnetoresistance*

1. Introduction

Metal-semiconductor multilayers (Mls) have been extensively studied because of their potential application in electronics. Recently the investigations have been focused on Fe/Si/Fe coupled heterostructures, since they show a very strong antiferromagnetic (AF) interlayer coupling [1, 2]. In spite of many efforts, the origin of the interlayer coupling in Fe/Si system has not been clarified. Moreover, it is not well understood how the formation of iron silicides affects the interlayer coupling. Therefore the information about the interface structure and its correlation with magnetic

*Corresponding author, e-mail: Lucinski@ifmpan.poznan.pl.

properties of this system is of particular interest. Compared to the extensive studies of Fe/Si systems there are relatively few reports discussing Co/Si systems [3–5]. The interlayer coupling in Co/Si was found to be antiferromagnetic between 0.8 and 1.7 nm. In this contribution we present the results of the magnetic studies of Fe/Si and Co/Si Mls.

2. Experimental

The $\{Fe(d_{Fe})/Si(d_{Si})\}_{15}$ + $Fe(d_{Fe})$, $\{Fe(d_{Fe})/Fe_{33}Si_{66}(d_{Fe_{33}Si_{66}})\}_{15}$ + $Fe(d_{Fe})$, and $\{Co(d_{Co})$ /$Si(d_{Si})\}_{15}$ + $Co(d_{Co})$ Mls were deposited by d.c. magnetron sputtering at room temperature (RT) onto SiO_x wafers. The crystalline structure of samples and their periodicity were examined using the high- and small-angle X-ray diffraction, HAXRD and SAXRD, respectively, whereas the interface structure of the Fe/Si Mls were studied by conversion electron Mössbauer spectroscopy (CEMS). Magnetization measurements were performed at RT using a vibrating sample magnetometer and magnetooptical Kerr effect (MOKE).

3. Results and discussion

3.1. Fe/Si and Fe/$Fe_{33}Si_{66}$ multilayers

Figure 1 shows examples of the field dependence of the Fe/Si magnetic moment of Mls with d_{Fe} = 3 nm for different Si thicknesses. As can be seen, the magnetic parameters like the remnant (M_R) to saturation (M_S) magnetization ratio (the so-called $F_{AF} = 1 - M_R/M_S$ parameter) and saturation field (H_S) are strongly influenced by Si spacer thickness. The F_{AF} parameter may indicate (or may be proportional to) the existence of the AF coupled fraction of Fe/Si Mls. $F_{AF}(d_{Si})$ dependence shows that the AF coupling occurs only for $1 \le d_{Si} \le 1.5$ nm and is centred at about d_{Si} = 1.4 nm where F_{AF} = 0.9 (Fig. 2). The same dependence and the occurrence of only single maximum of F_{AF} are reproduced by $H_S(d_{Si})$. For d_{Si} = 1.4 nm H_S reaches its maximum value of about 1.5 T which may be ascribed, according to the relation $J = (1/4)H_S M_S d_{Fe}$, to the occurrence of a very strong AF interlayer coupling $J = -1.93$ mJ/m^2. Above d_{Si} = 1.4 nm saturation fields decay exponentially and for thicker Si spacer no additional H_S peaks were found up to d_{Si} = 5 nm. For $d_{Si} > 1.5$ nm both F_{AF} and H_S values are strongly reduced, $F_{AF} < 0.5$ and $H_S < 0.1$ T. The reduction of F_{AF} and H_S values for $d_{Si} < 1.4$ nm points out that the neighbour Fe layers become gradually connected through pinholes. The observed non-oscillatory but exponentially decaying saturation field values (see inset in Fig. 2) seem to correspond to the quantum interference model of exchange coupling [6].

Figure 3 displays SAXRD and HAXRD spectra for d_{Fe} = 3 nm and d_{Si} = 1.4 nm. SAXRD pattern proves a very well layered structure of the Mls with four superlattice peaks indicating strong composition modulation along the growth direction. The in-

tense peak near 70° (and all underlined refraction indexes) in the HAXRD spectrum is due to the Si substrate. Only one weak satellite peak is visible near bcc (110), in contrast to Fullerton [6], who observed satellite peaks around the Fe (110). However, this is in agreement with Chaiken [7], who observed only one satellite peak on the low-angle side of Fe (110) peak.

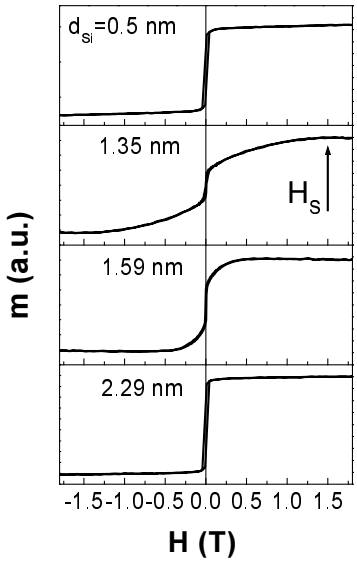

Fig. 1. Examples of the Fe/Si magnetic moment field dependencies of Mls with fixed d_{Fe} = 3 nm and different Si thicknesses

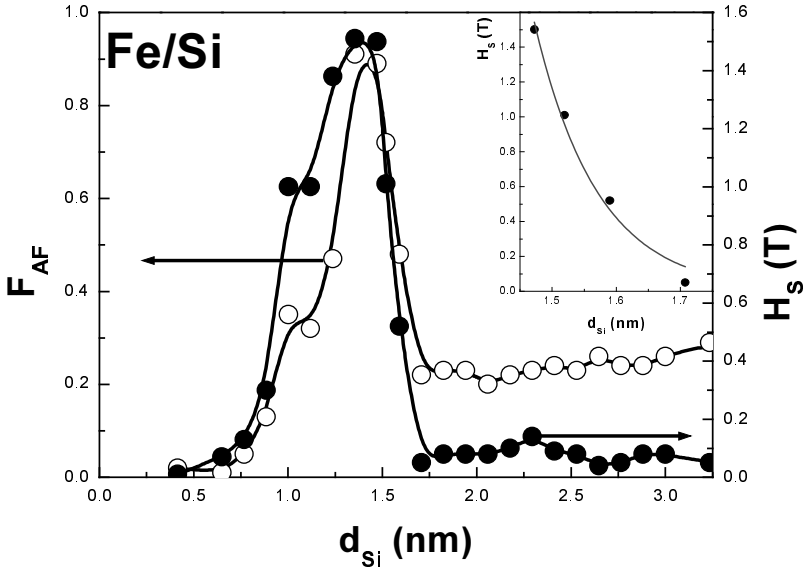

Fig. 2. Values of F_{AF} parameter, the saturation fields H_S versus d_{Si} for Fe/Si Mls with d_{Fe} = 3 nm. The inset shows the exponential decay of H_S as a function of d_{Si}

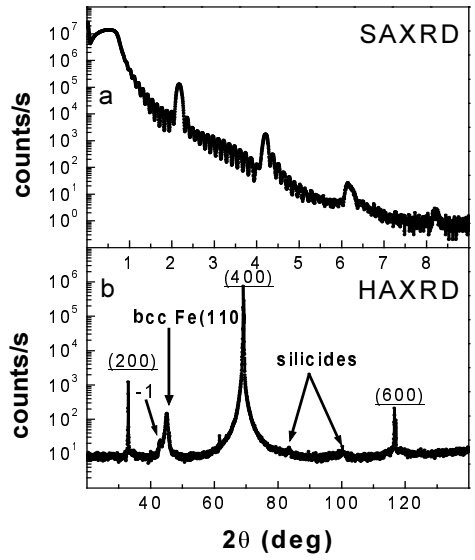

Fig. 3. Two typical small- (a) and high-angle (b) XRD spectra (SAXRD and HAXRD, respectively) for Fe/Si Ml with the strongest interlayer coupling (d_{Fe} = 3 nm and d_{Si} = 1.4 nm)

Our XRD measurements did not show any clear evidence of iron silicides formation at Fe/Si interfaces. Only two tiny peaks around 84° and 100° suggest the presence of Fe–Si phases. The absence of Fe–Si silicides in HAXRD spectra does not exclude their existence in Fe/Si Mls, but suggests that their volume fraction is very small. The possible candidates are nonmagnetic metallic phases of tetragonal α-$FeSi_2$ (and/or a semiconducting β-$FeSi_2$) and FeSi with CsCl structure.

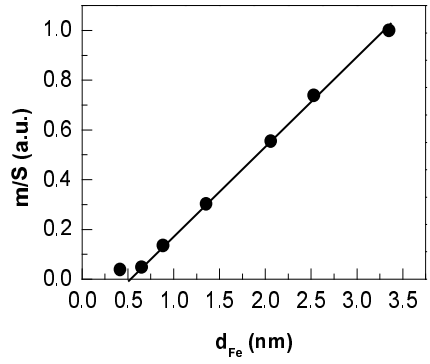

Fig. 4. Fe thickness dependence of magnetic moment per surface area (m/S) for Fe/Si Mls with constant d_{Si} = 2.5 nm

Figure 4 shows the Fe thickness dependence of magnetic moment per surface area (m/S) for Mls with d_{Si} = 2.5 nm. The relationship between m/S and d_{Fe} can be described by $m/S = M_0(1 - 2d_0/d_{Fe})$, where M_0 is an average magnetization of Fe layers and d_0 is an effective dead layer per single Fe/Si interface. The intercept of the straight line with d_{Fe} axis gives the thickness of nonmagnetic layers showing that about 0.25 nm thick nonmagnetic layer is formed at each Fe/Si interface. This may be ascribed to the intermixing of Fe and Si leading to the formation of thin nonmagnetic Fe–Si interfacial phases.

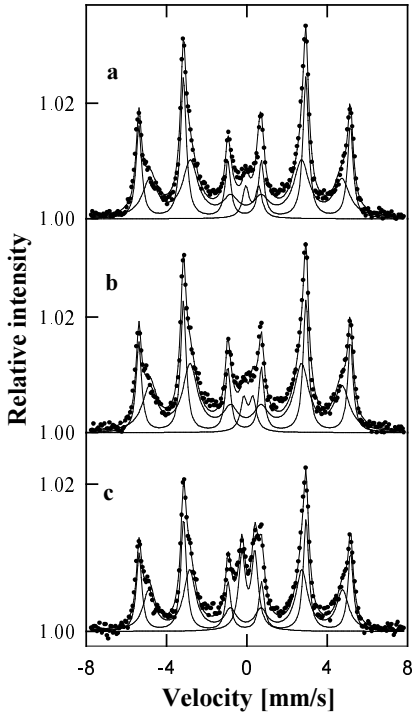

Fig. 5. CEMS spectra of Fe/Si Mls with Si layer thickness of 1.2 nm (a), 1.4 nm (b) and 2.3 nm (c), respectively

To gain more information on the interface structure, CEMS measurements have been performed for the Fe/Si Mls with constant d_{Fe} = 3 nm and $1.2 \le d_{Si} \le 2.3$ nm. The CEMS spectra recorded at room temperature consist of the Zeeman sextet with narrow lines ($\Gamma \approx 0.32$ mm/s) and with the hyperfine field $H_{hf} \approx 32.8$ T and isomer shift IS = 0.00 mm/s, characteristic of the pure bcc-Fe phase, and of two spectral components related to the FeSi system: magnetic broad sextet and nonmagnetic quadrupole doublet (Fig. 5a–c). The broad sextet ($H_{hf} \approx 29$ T and $IS \approx 0.05$ mm/s) originates most probably from Fe atoms placed at various sites at the interface surrounded by Si atoms. The Fe atoms are located in a crystalline bcc phase surrounded by seven Fe atoms and one Si atom [8]. The spectral contribution of this sextet does not change significantly for various d_{Si} and contributes in about 50% to the total spectral area (Fig. 5). The nonmagnetic component, consisting of the quadrupole doublet (QS) with the quadrupole splitting of about 0.64 mm/s and isomer shift $IS \approx 0.20$ mm/s, could originate either from the ε-FeSi nonmagnetic small-gap semiconductor with a cubic symmetry or from the crystalline c-$Fe_{1-x}Si_x$ metallic metastable phase with a CsCl structure [9]. Stoichometric c-FeSi phase, having a cubic structure, usually exhibits a single-line Mössbauer spectrum but, as shown by Strijkers [9], when Fe vacancies are introduced, a quadrupole splitting is observed. Furthermore, also strain in the layer reduces local symmetry introducing electric field gradient. Our spectral parameters of the QS doublet could also be related to the α-$FeSi_2$ or β-$FeSi_2$ phases. Our QS value of about 0.64 mm/s could correspond to the poorly resolved doublets with QS_1

= 0.47 mm/s and QS_2 = 0.73 mm/s of the α-$FeSi_2$ phase with a tetragonal structure [9, 10]. However, the QS values of β-$FeSi_2$ [11] are considerably smaller than those found in our CEMS spectra and therefore the presence of β-$FeSi_2$ phase could be excluded. The spectral contribution of the QS doublet increases from about 5.7% for $d_{Si} \leq 1.35$ nm (Fig. 5a) to about 16% for $d_{Si} = 2.3$ nm (Fig. 5c). Since the QS doublet is a minor spectral component, it is difficult to identify clearly from the QS and IS values which FeSi-type phase appears in our Fe/Si Mls; however, the c-$Fe_{1-x}Si_x$ one seems to be more plausible.

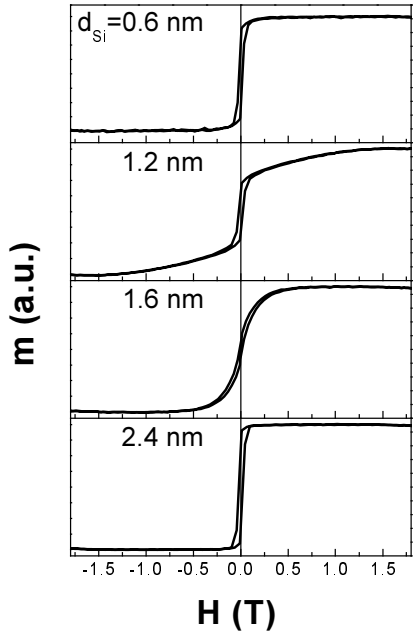

Fig. 6. Exemplary $m(H)$ loops for Fe/$Fe_{33}Si_{66}$ Mls for $d_{Fe} = 3$ nm and for different $Fe_{33}Si_{66}$-spacer layer thickness

In order to check the influence of Fe addition in Si spacer on H_S, we prepared $\{Fe(3nm)/Fe_{33}Si_{66}(d_{Fe_{33}Si_{66}})\}_{15}$ + Fe(3*nm*) Mls, with $Fe_{33}Si_{66}$ simulating the $FeSi_2$ phase. Figure 6 shows some examples of $m(H)$ loops and Fig. 7 displays the values of the F_{AF} and the H_S versus $d_{Fe_{33}Si_{66}}$. Comparing Fig. 2 and Fig. 7 one can realize that in the case of $Fe_{33}Si_{66}$-spacer layer, F_{AF} is reduced and its maximum is shifted towards thicker spacer layers values. Simultaneously, the position of the H_S maximum is almost unchanged; however, its value is visibly reduced from 1.5 (for Fe/Si Mls) to 1.3 T. The observed shift of the F_{AF} maximum value towards thicker spacer layers with unchanged position of H_S suggests the influence of pinholes for $d_{Fe_{33}Si_{66}} < 1.5$ nm. Similarly to Fe/Si Mls saturation fields for $d_{Fe_{33}Si_{66}} > 1.2$ nm decays exponentially (inset in Fig. 7) showing no oscillatory behaviour. Due to the appearance of ferromagnetic coupling at small spacer layer thickness (Fig. 2 and Fig. 7) attributable to the pinholes formation and very weak coupling observed above H_S peaks, the thickness dependence

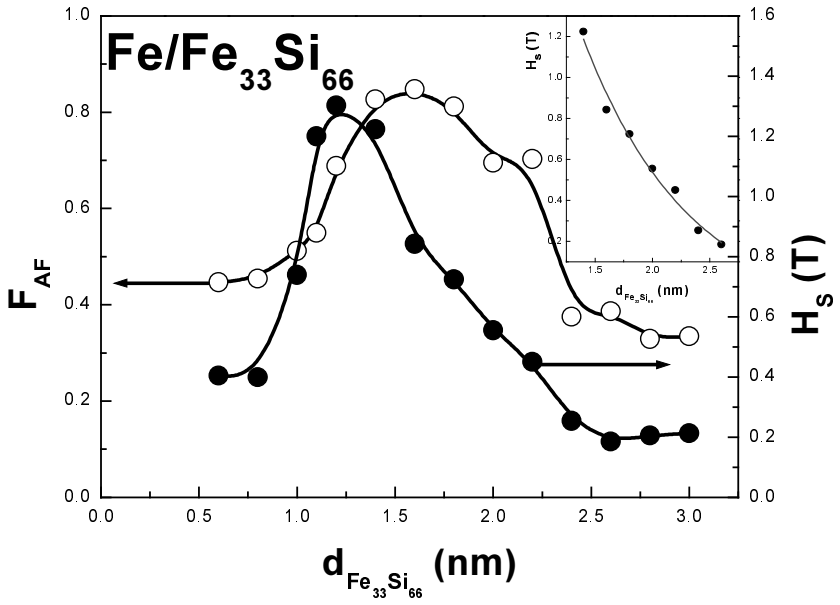

Fig. 7. The values of F_{AF} parameter and H_S field for Fe/$Fe_{33}Si_{66}$ Mls as a function of $d_{Fe33Si66}$ for constant d_{Fe} = 3 nm. The inset shows the exponential decay of $H_S(d_{Fe33Si66})$

of H_S across Si and $Fe_{33}Si_{66}$ spacers may be misread as a single maximum of an oscillation. Comparing the results obtained for Fe/Si and Fe/$Fe_{33}Si_{66}$ Mls we can conclude that the exchange coupling is distinctly stronger for nominally pure spacer layer.

3.2. Co/Si multilayers

In Co/Si Mls, a negative heat of mixing between Co and Si results in the formation of metastable amorphous phases and to the mutual solubility of constituents (see [4, 5] and references therein). This may be responsible for very complex and unusual magnetic behaviour. To our knowledge till now there was no detailed search for AF coupling in sputtered Co/Si Mls except the short information given in abstract [3] about the range of such a coupling.

Figure 8 displays examples of SAXRD and HAXRD spectra for d_{Co} = 3 nm and d_{Si} = 2.8 nm. SAXRD pattern proves a very well layered structure of the Mls with four superlattice peaks. All underlined refraction indexes in HAXRD are due to the Si substrate.

Figure 9 shows the MOKE loop shape variation of Co(d_{Co})/Si(2.4 nm) Mls for different d_{Co} in two magnetic field directions in Ml plane. One can immediately realize that character of the $m(H)$ traces depends on d_{Co}. We connect it with the evolution of the Co layer from superparamagnetic granular structures for $d_{Co} \leq 1$ nm through dis-

continuous granular Co layer for $1< d_{Co}\leq 2$ nm and finally to continuous Co layer for $d_{Co} \geq 2.2$ nm. Figure 10 displays the Co thickness dependence of the sample moment per surface area (m/S). We have found that nominally about 0.25 nm thick layer per single Co/Si interface is magnetically inactive. However, in contrast to Fe/Si Mls, the character of the $m/S(d_{Co})$ is more complex revealing a drastic transition from discontinuous to continuous structure of Co layers at about d_{Co} = 2 nm. Such a behaviour suggests that the growth of Co on Si occurs in an island growth mode.

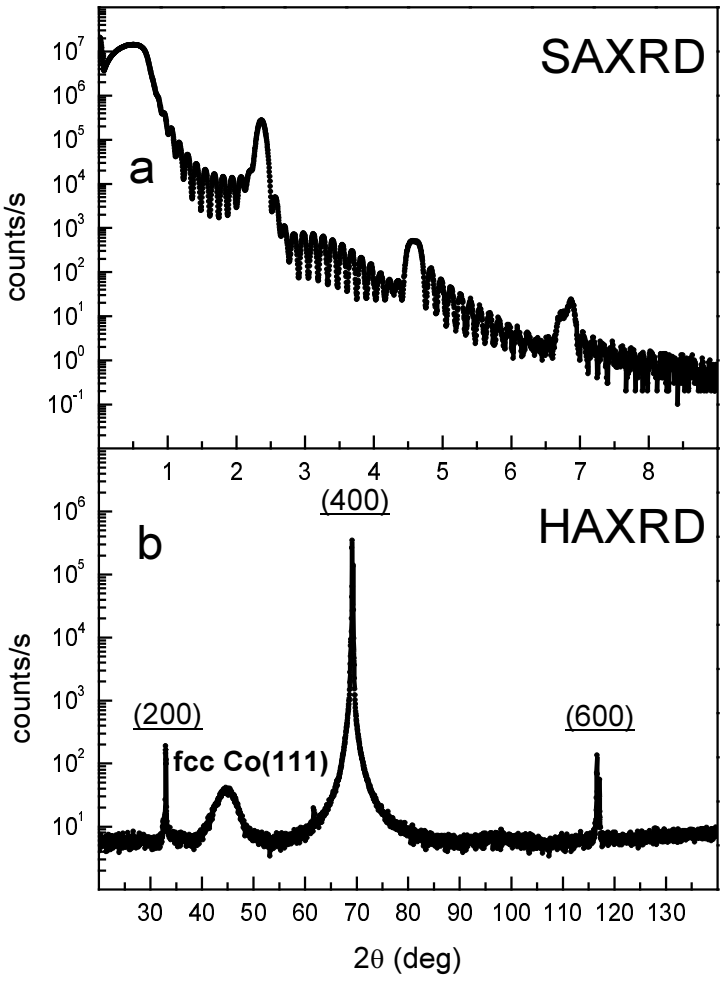

Fig. 8. Two typical small- (a) and high-angle (b) XRD spectra (SAXRD and HAXRD, respectively) for Co/Si Ml with d_{Fe} = 3 nm and d_{Si} = 2.8 nm

Figure 11 shows the evolution of MOKE $m(H)$ loops for Co(3*nm*)/Si(d_{Si}) versus Si thickness for selected samples. Such behaviour implies the existence of a weak

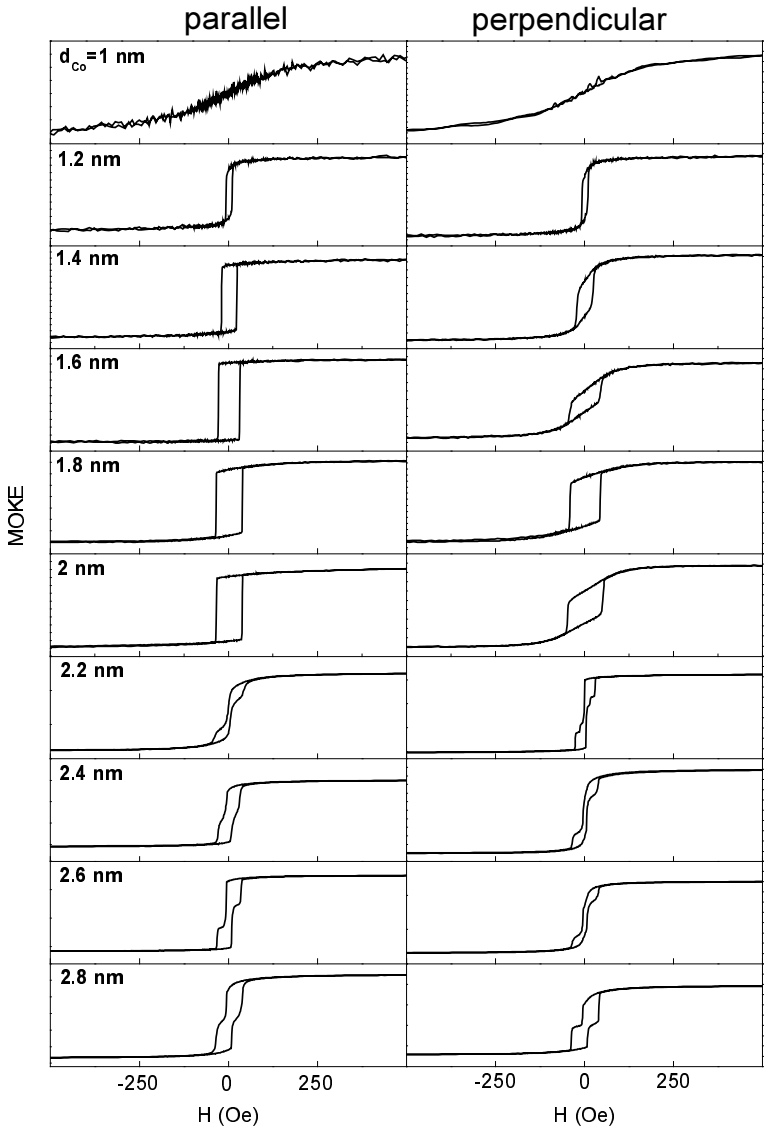

Fig. 9. The examples of $m(H)$ loops measured by MOKE for two perpendicular magnetic field directions in the sample plane for Co(d_{Co})/Si(2.4 nm) for different Co layer thickness

interlayer coupling that modifies the hysteresis loop shapes from square-like to step-like characterized by two "coercive" fields: H_{C1} and H_{C2}. This seems to be confirmed by the $F_{AF}(d_{Si})$ oscillatory dependence presented in Fig. 12a (top panel). Due to a very weak coupling the correct identification of the saturation fields was very difficult. Therefore in Fig. 12b we present the values of H_{C1} and H_{C2} fields as a function of Si

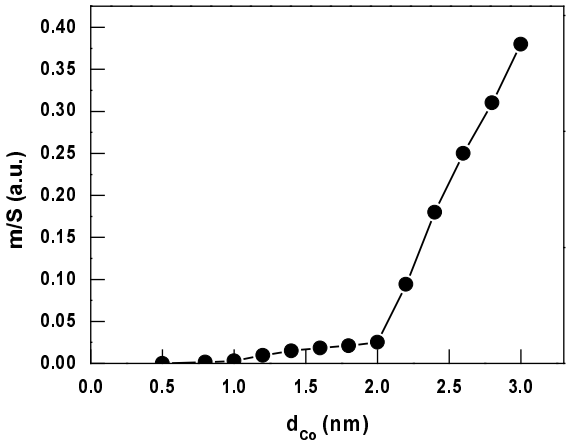

Fig. 10. Co thickness dependence of magnetic moment per surface area (m/S) of Co/Si Mls with constant d_{Si} = 2.8 nm

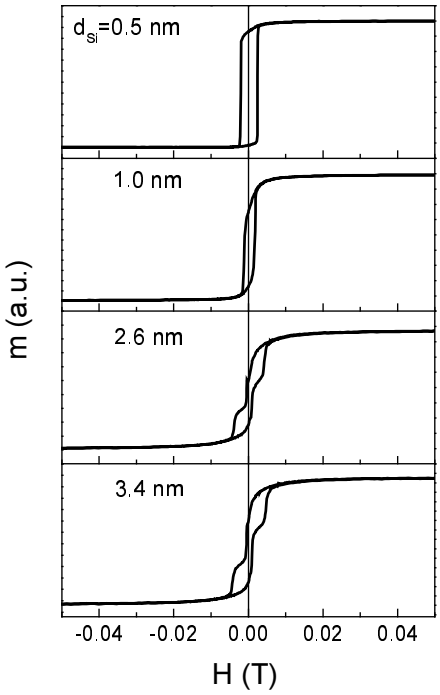

Fig. 11. The evolution of $m(H)$ loop shapes as a function of Si sublayer thickness for Co/Si Mls with d_{Co} = 3 nm

thickness. From this figure one can see that H_{C2} appears only for thicker Si layers, i.e., for $d_{Si} \geq 1.5$ nm. Below this Si thickness only single, almost square-shaped loops ap-

pear. Such $m(H)$ behaviour can be explained by a simple model describing the total magnetic energy of bilayer:

$$E = -M_S H d_{\mathrm{Co}} (\cos\varphi_1 + \cos\varphi_2) + J\cos(\varphi_1 - \varphi_2) + 0.25 K d_{\mathrm{Co}} (\sin^2\varphi_1 + \sin^2\varphi_2)$$

where $\varphi_{1(2)}$ are the angles between the applied field H and magnetizations, and J and K denote the interlayer coupling and cubic anisotropy, respectively.

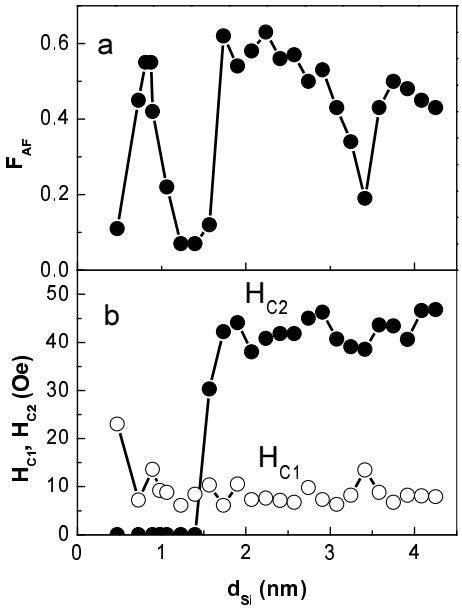

Fig. 12. Si thickness dependence of F_{AF} parameter (a) and two characteristic fields H_{C1} and H_{C2} (b) for Co/Si Mls

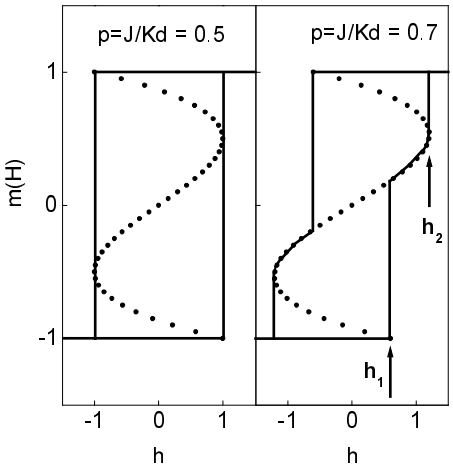

Fig. 13. Visualization of $m(H)$ model hysteresis loop shapes for different coupling to anisotropy J/Kd_{Co} ratios. h_1 and h_2 fields represent spin-flip and spin-flop fields, respectively. The dotted line represents $\partial E/\partial m = 0$ (see text)

It can be shown that for low interlayer coupling, i.e., for $p = J/Kd < 0.5$, the effective exchange coupling is so weak that the anisotropy controls the switching characteristics and as a result square loops appear (Fig. 13). For $0.5 < p = j/Kd < 1$, two characteristic fields emerge: $h_1 = -2(p - 1)$ and $h_2 = 8[(p + 1)/6]^{3/2}$, where $h = HM_S/K$. The dotted line in Fig. 13 represents $\partial E/\partial m = 0$ where $m = \cos(\varphi_1 - \varphi_2)$. Both small value of the F_{AF} parameter and simple square $m(H)$ loops observed for the sample in the vicinity of the first $F_{AF}(d_{\mathrm{Si}})$ maximum suggest the presence of the magnetostatic coupling. Its source most probably is in the pinholes formation which reduces the AF exchange coupling in this d_{Si} range. The observed $F_{AF}(d_{\mathrm{Si}})$ oscillatory behaviour suggests that the Co–Si nonmagnetic metallic phases replace nominally

pure Si-spacer layers, since the oscillatory behaviour points to the RKKY-like type of interlayer coupling via conduction electrons.

3.3. Application of strongly coupled Fe/Si multilayers

Since the strongest AF interlayer coupling in our Fe(3*nm*)/Si Mls has been found for d_{Si} = 1.4 nm, it was very interesting to find out whether it can be applied as an artificial antiferromagnet in magnetoresistive $(Fe/Si)_{15}$/Fe/Co1/Cu/Co2 pseudo-spin –valve (PSV) system. We used a Co1/Cu/Co2 trilayer as the magnetoresistive structure with Co1(2) and Cu thicknesses of about 1.5 nm and 2.5 nm, respectively.

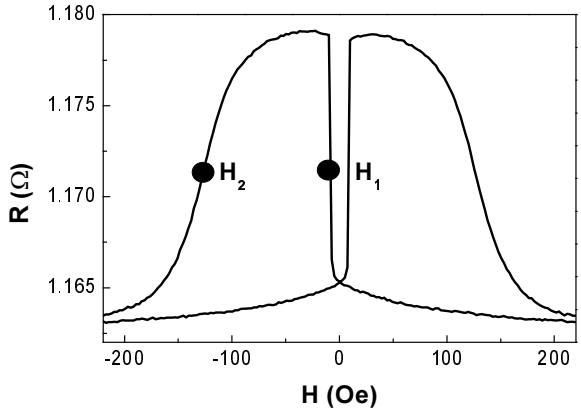

Fig. 14. Magnetoresistance effect of $(Fe/Si)_{15}$/Fe/Co1/Cu/Co2 pseudo-spin–valve system, where Fe/Si Ml was used as an artificial antiferromagnet

Since the last Fe and the Co1 layers are in the intimate contact, the Fe/Co1 bilayer behaves as a first magnetoresistive layer in the examined structure. The field dependence of the sample resistance, shown in Fig. 14, reflects a typical PSV giant magnetoresistance behaviour. As can be seen, there are two switching fields: H_1 related to the magnetization reversal of the top Co2 layer and H_2 due to switching of the Fe/Co1 pinned bilayer magnetization to the direction of the external magnetic field at higher fields. Since Fe/Co1 bilayer is AF coupled to the rest of Fe/Si Ml structure, it reverses at higher fields – the top Co2 layer and an AF arrangement between magnetizations of the Fe/Co1 bilayer and the Co2 layer occurs between H_1 and H_2.

4. Conclusions

Magnetic and structural properties of Fe/Si, $Fe/Fe_{33}Si_{66}$ and Co/Si Mls have been examined. For Fe/Si Mls very strong AF coupling (J = –1.93 mJ/m^2) has been found for Si thickness of about 1.4 nm and magnetic moment measurements revealed that

0.25 nm of Fe per single interface is magnetically inactive. The interface structure of Fe/Si Mls, studied by CEMS, suggests that the c-$Fe_{1-x}Si_x$ was formed at the interfaces. Comparing the results obtained for Fe/Si and Fe/$Fe_{33}Si_{66}$ Mls we conclude that the AF coupling is distinctly stronger for nominally pure spacer layer. In both kinds of Mls, only single H_S maximum versus spacer-layer thickness was observed and H_S values decay exponentially above the maximum. For Co/Si Mls a very weak AF coupling and oscillatory $F_{AF}(d_{Si})$ behaviour were observed most probably due to the Co–Si nonmagnetic metallic phases formation replacing nominally pure Si spacer layers. Magnetic moment measurements showed that the growth of the Co on Si occurs in an island-growth mode in contrast to Fe/Si Mls. We have shown that the evolution of magnetic loop shapes can be successfully explained by the interplay between J and Kd.

We have shown that AF coupled Fe/Si Mls can be applied as an artificial antiferromagnet in magnetoresistive pseudo-spin–valve system.

Acknowledgements

This work has been supported by the KBN (Poland) under grant No. PBZ/KBN-013/T08/23 and PBZ/KBN/044/PO3/2001.

References

[1] GAREEV R.R., BÜRGLER D.E., BUCHMEYER M., OLLIGS D., SCHREIBER R., GRÜNBERG P., Phys. Rev. Lett., 87, (2001), 157202.
[2] GAREEV R.R., BÜRGLER D.E., BUCHMEYER M., SCHREIBER R., GRÜNBERG P., J. Magn. Magn. Mater., 240 (2002), 235.
[3] INOMATA K., SAITO Y., J. Appl. Phys., 81 (1997), 5344.
[4] GRUNDY P.J., FALLON J.M., BLYTHE H.J., Phys. Rev., B62, 9566 (2000).
[5] FALLON J.M., FAUNCE C.A., GRUNDY P.J., J. Appl. Phys., 88, 2400 (2000).
[6] FULLERTON E.E., MATSON J.E., LEE S.R., SOWERS C.H., HUANG Y.Y., FELCHER G., BADER S.D., PARKER F.T., J. Magn. Magn. Mater., 117 (1992), L301.
[7] CHAIKEN A., MICHEL R.P., WALL M.A., Phys. Rev., B 48 (1996), 5518.
[8] DUFOUR C., BRUSON A., MARCHAL G., GEORGE B., MANGIN PH., J. Magn. Magn. Mater., 93 (1991), 545.
[9] STRIJKERS G.J., KOHLHEPP J.T., SWAGTEN H.J.M., DE JONGE W.J.M., Phys. Rev., B 60 (1999), 9583.
[10] HELGASON O., SIFUSSON T.I., Hyperfine Interact., 45 (1989), 415.
[11] MILOSAVLJEVIC M., DHAR S., SCHAAF P., BIBIC N., HUANG Y.-L., STEIBT M., LIEB K.P., J. Appl. Phys., 90 (2001), 4474.

Received 4 December 2002